# Carbonization of Cellulose in Supercritical $CO_2$ for Value-Added Carbon

**Kiran G. Burra**
The Combustion Laboratory,
Department of Mechanical Engineering,
University of Maryland,
College Park, MD 20742
e-mail: kiranraj@umd.edu

**Nick Daristotle**
The Combustion Laboratory,
Department of Mechanical Engineering,
University of Maryland,
College Park, MD 20742
e-mail: nickdari@terpmail.umd.edu

**Ashwani K. Gupta**
The Combustion Laboratory,
Department of Mechanical Engineering,
University of Maryland,
College Park, MD 20742
e-mail: akgupta@umd.edu

*In this paper, carbonization of biomass in the presence of supercritical $CO_2$ is investigated to obtain carbon solids with enhanced properties and potential to provide a sustainable pathway for high-value solid products which are currently resourced from expensive and carbon driven fossil-fuel routes. Carbonization of cellulose was carried out in supercritical $CO_2$ at temperatures of 523 K and 623 K at ~100 bar pressure in a stirred reactor for 1–8 h of residence times. The obtained solid residue was characterized for morphology using scanning electron microscopy (SEM), surface graphitization using Raman spectroscopy, thermal stability using thermogravimetric analysis (TGA), and crystallinity using powder X-ray diffraction (XRD). The solid chars were found to be dominated by clusters of microspheres (<5 μm), especially at temperatures of 623 K. Raman spectroscopy revealed the formation of graphitic crystallite units connected by $sp^3$ carbons (i.e., aliphatic) suggesting significant graphitization. G-band peak ratio was found to be highest for a residence time of 5 h for both the temperatures. TGA data revealed that higher carbonization temperature led to higher thermal decomposition peaks of the chars. The peak value of thermal decomposition ranged between 700 and 800 K for char obtained at 523 K and between 750 and 900 K for char at 623 K. The values were significantly higher than the decomposition peak cellulose at ~610 K. Proximate analysis results revealed significant increase of fixed carbon content compared with cellulose. Fixed carbon to volatile content ratios revealed increase from 0.052 in cellulose to values ranging from 1.4 to 4.3 making these chars similar in character to coal (with ranking of bituminous coal and petroleum coke). The net yield of solid chars from carbonization was around 50–66% depending upon the extent of carbonization. These results suggest this pathway to produce high yields of high-quality carbon solids with low volatile content, high thermal stability, and significant graphitization. The graphitized carbon offers potential applications in catalysis, electrode materials, pollutant absorption, and energy storage and solid fuels while avoiding drying to remove moisture unlike pyrolysis.* [DOI: 10.1115/1.4050634]

*Keywords: supercritical $CO_2$, carbonization, cellulose, high-value carbon, carbon microspheres, alternative energy sources, energy extraction of energy from its natural resource, energy from biomass, energy storage systems*

## 1 Introduction

Municipal solid wastes (MSWs) have been increasing while their management has been limited to landfilling along with some level of recycling [1]. Thermochemical pathways such as pyrolysis, gasification, and incineration have been proposed to support their management along with biomass resources such as agricultural and forestry residues, energy crops, manure, and other low-grade biowastes via conversion for energy production [2]. But, high water and ash content, heterogeneity in the biomass feedstocks means that energy produced from these resources is of lower economic value. This is a major drawback for the sustainable upscaling of these thermochemical pathways. To address this issue of low-economic output, a promising strategy has been proposed involving the production of products of high economic value from these wastes, with sufficient yields to support the low-value and high-yield products such as energy production. This strategy can effectively allow for better economic viability and technical feasibility for sustainable disposal and utilization of the biomass and MSW resources. High-value products could include the production of aromatic chemicals such as benzene, toluene, or 5-hydroxymethylfurfural (5-HMF), and higher alcohols, but their production is subjected to severe contamination in the form of byproducts owing to the diverse composition of biomass and the products obtained from fast-pyrolysis, while biochemical pathways severely limit the upscaling in terms of feedstock compatibility [3–5].

Solid carbonaceous material production is a better pathway as it can provide relatively uniform properties along with the versatile applicability of these products [6]. This typically involves carbonization of feedstocks in different types of conditions to obtain char with enhanced carbon content, improved energy density, and increased crystalline order depending on the severity of the process. Macro products of interest range from mesoporous activated carbon and its derivatives loaded with metal nanoparticles, char with high-graphitic content for electrochemical and energy storage applications, good-quality solid carbon fuels to support coal, and coke for metallurgical applications [6,7]. In addition, other high-quality novel products include graphene layer extraction, graphene, and carbon quantum dots with various applications including biomedical imaging, electrochemical and semi-conductor materials, although the production of these materials required additional processing of the carbonized solids [8–10]. Pyrolysis close to atmospheric pressures and high temperature (>973 K) has been carried out by various researchers to carbonize biomass and MSW to produce activated carbon via physical and chemical activation, high carbon content, and graphene extraction from activated carbon [8,11–13]. While the quality of the products has been

Contributed by the Advanced Energy Systems Division of ASME for publication in the Journal of Energy Resources Technology. Manuscript received January 8, 2021; final manuscript received March 21, 2021; published online April 22, 2021. Editor: Hameed Metghalchi.

established to be scalable, pyrolysis is limited due to significantly low yields since the high volatile content in the feedstocks used results in major carbon-loss in volatile form.

Alternative, high-pressure pyrolytic techniques have been investigated which include solvothermal process such as hydrothermal carbonization (HTC) and other supercritical solvent based carbonization techniques [14–17]. HTC involves carbonization of the feedstock in the presence of water at temperatures of 400–750 K and autogenic pressures greater than 100 bar to reach near-critical water conditions for residence times ranging from 1 to 24 h. Literature reports are available from investigations into various kinds of biomass and waste feedstocks (such as monosaccharide solutions such as glucose, levulose, and starch), lignocellulosic components (such as cellulose, xylan, and lignin), algal biomasses, municipal waste streams (such as paper, cardboard, food, and other organic MSW), anaerobic digestion waste, sewage sludge, and other agricultural and forestry biomasses [18–23]. Extensive research can be found with significant knowledge on the effect of operating conditions (temperature, pressure, residence time, solvents, and additives such as alcohols, and ammonia, and pH variation from the addition of citric acid), feedstock type and loading on the characteristics of solid residues after it is filtered and dried [24–26]. Solid residue from HTC, also called hydrochar, obtained from cellulose was found to have combustion characteristics similar to subbituminous coal and this showed similarity for different types of feedstocks examined [21,27,28]. The morphology of hydrochar obtained from monosaccharides was found to contain uniform carbon microspheres (1–5 $\mu$m). These microspheres and their cluster forms were also observed from the conversion of cellulose and other biomass feedstocks [29–32]. Mechanistic understanding revealed that under hydrothermal conditions, saccharides initially underwent dehydration reactions leading to polymerization of anhydrides to form carbon nanospheres [14,24]. The colloid of these carbon nanospheres further undergoes condensation to form carbon microspheres to reduce the interfacial energy [14]. The addition of acids such as citric acid was found to improve the dehydration reaction leading to increase in microsphere size [24]. The aromatic rings condensed to form graphitic crystallite content which were connected by $sp^3$ (aliphatic compound which offers mixing of one s atomic orbital with three p atomic orbitals) carbon bonds while the oxygenate content, facing outward from the centers of microspheres, leads to hydrophilic residue [32,33]. The hydrochar obtained from this was investigated for suitability in various applications including activated carbon, graphene layers and quantum dots, anode for lithium-ion batteries, and metal-doped carbon catalysts. Although there is significant interest in HTC to produce high-value carbon materials, the water obtained after HTC contains carcinogenic components and tar components that required their cleaning before disposal [6,7,34]. In addition, since the hydrochar is hydrophilic, their filtration from the water and extensive cleaning and drying potentially limits its scalability. To counter these issues, we examine the replacement of near-critical water with supercritical $CO_2$ to effectively perform supercritical $CO_2$-assisted carbonization of biomass and waste feedstocks to obtain high-value char products, and thus also utilizing $CO_2$.

$CO_2$ is a relatively inert and nontoxic, non-flammable feedstock which is readily available as flue gas at low cost while its low-critical point (304.1 K and 7.38 MPa) makes its production significantly easier compared with other supercritical fluids such as water and alcohols. Low and gas-like viscosity, with high density, zero surface tension and high diffusion capabilities of supercritical $CO_2$ along with its quadrupole moment, and polar C=O bonds makes it an effective non-polar solvent while also dissolving functional groups such as –OH, –F, and –CO [35]. Although it does not dissolve very polar compounds such as water, sugars, and inorganic salts, the literature reveals that water can form emulsion in supercritical $CO_2$ by stabilizing this emulsion using surfactants, especially amphiphilic surfactants (Ex: perfluoropolyether, Na-bis(2-ethylhexyl) sulfosuccinate) which can be useful in various nanomanufacturing applications [35]. While the major industrial applications currently are limited to thermal power plants and in the food industry (decaffeination, hops, and cork extraction), interest in its applicability toward nanoparticles and novel material manufacturing has been increasing in recent times owing to increased interest in novel materials and pathways for their sustainable production [35–39].

Currently researched solvent applications of supercritical $CO_2$ include polymer and extractant purifications via residual solvent removal. Note that its density tunability and non-polar solvent characteristics make it useful for polymerization reactions [36,40]. As $CO_2$ is a gas at STP, these residuals can be easily precipitated while the $CO_2$ can be reused. This has also been used to regenerate absorbents and porous catalysts as the organic residues inside these materials can be effectively removed compared with other methods such as steam stripping without leaving any residual solvent to provide enhanced regeneration of absorption capacity and catalyst activity [36]. This high regenerative capability makes it a very attractive solvent to provide green and sustainable routes for these applications. Supercritical $CO_2$ conditions have also been utilized to produce polymeric foams due to its easier diffusivity allowing for porous polymer production while also providing control over the pore size and growth [40–43]. Zero surface tension of supercritical $CO_2$ was also utilized for novel drying applications such as cleaning of microelectromechanical systems (MEMS) to remove organic residuals and effective drying of cellulosic and silica aerogels while maintaining crystalline size and avoiding agglomeration that can occur via other harsher routes [35].

Supercritical $CO_2$ has also been proposed and investigated for nanoparticle synthesis as it can provide products with low defects to replace expensive routes that need precious raw materials and harsher chemicals [36]. The effective solubility and control of other properties via tuning the operating conditions of supercritical $CO_2$ makes it attractive for these applications to provide precision synthesis while lowering solvent, energy, and material costs. It was used for graphite exfoliation to produce mono and multi-layer graphene which can provide effective and sustainable pathway to produce this high-value material without the need for harsh chemicals such as $H_2SO_4$ and HCl needed for conventional graphene exfoliation processes [44,45]. In addition, emulsions of supercritical $CO_2$ containing metal precursors were also utilized effective impregnation of nanoporous substrates such as carbon nanotube walls owing to its high density and diffusivity, low viscosity, and zero surface tension for deeper penetration while ensuring the structural integrity of these nanopores to provide metal-doped carbon nanotubes [35].

Promising pathways have been reported for sustainable material production via supercritical $CO_2$ utilization. The use of supercritical $CO_2$ for solvothermal carbonization from its non-polar solvent capabilities can improve condensation reactions while the non-polar tar products can be easily separated and dissolved in supercritical $CO_2$, which makes it a better pathway as compared with HTC. This pathway can also provide the use of $CO_2$ resulting in more carbon utilization, which then also lowers carbon emission into the atmosphere. But research into this aspect has been sporadic and limited [46]. Moreover, its utilization to deal with biomass and low-grade wastes for simultaneous carbonization and drying has not been investigated while its involvement in biomass processing has been limited to breaking down of cellulose fibers at low temperature as a pretreatment for enzymatic conversion [47,48]. These rare investigations into carbonization of components of biomass and MSW in the presence of supercritical $CO_2$ have been carried out using plastics such as polyethylene (PE), polyvinylchloride (PVC), polypropylene (PP), polyvinylidene chloride (PVDC), and polyethylene terephthalate (PET) [14]. This has been carried out in the presence of supercritical $CO_2$ at high temperatures (773–973 K) and autogenic pressures (10–30 MPa) which resulted in the production of carbon microspheres at residence times as high as 20 h. In the case of PET conversion with a residence time of 3 h, byproduct analysis revealed that an increase in temperature led to breakdown of PET into aromatics (benzene and toluene) along with $CO_2$ and $H_2O$ [49]. These aromatics then dissolved in

supercritical $CO_2$. An increase in temperature and residence time led to condensation as clusters to form highly aromatic carbon microspheres (1–5 $\mu$m diameter). An increase in residence time and temperature was found to enhance graphitization and yield. A sufficient quantity of $CO_2$ was required to decrease irregularities and amorphous content on these microspheres. High temperatures led to morphological uniformity with carbon content in these spheres as high as 93% [49]. Morphological dependence on the PET's initial form was also found wherein the PET films produced carbon microspheres and crushed PET (150–250 $\mu$m) produced conglomerates of irregular spheres. In the case of PE conversion, flaky carbon deposits from carbonization of gas intermediates along with spheres from liquid carbonization were observed, while long residence times separated out these microspheres [14]. Lower temperature and shorter times led to the formation of polynuclear aromatic spheres. For PET, high temperatures were required for complete conversion to carbon microspheres as lower temperatures led to incomplete conversion and appearance of white waxy solids, possibly owing to the high pyrolysis temperatures of PET. Supercritical $CO_2$ was also used to convert hydrocarbons ($C_5$–$C_{14}$) at 973 K for 3 h in which it was proposed that C:H < 1 led to sufficient availability of H to cap the edges while C:H > 1 led to further polymerization into flakes [50]. It was suggested that clusters containing aromatic rings connected by aliphatic chains are the intermediates that form to minimize interfacial energy. They rearrange aromatics at the core while aliphatic tails are exposed to the solvent. Carbonization of discarded oil using supercritical $CO_2$ at $T > 773$ K revealed the formation of spheroids while further increase in temperature led to improved yield of spheres [51]. It was suggested that hydrophilic content in this provided the anisotropy and this carbonization led to the formation of graphene crystallites in the residue but with low levels of graphitization. While similar materials were also formed via high-pressure carbonization at high temperatures (>1073 K), the presence of supercritical $CO_2$ led to the formation of these materials at significantly lower temperatures [14].

The studies carried out at relatively high temperature ($T > 773$ K) and high-pressure conditions although produced novel materials, their scalability was limited by the requirement of special alloys, issues concerning safety, and feasibility, while alternative pathways to produce similar products are reported in the literature [14,52]. Supercritical $CO_2$ for carbonization at lower temperatures (450–700 K) and autogenic pressures can allow us to use existing reactor materials and conditions to allow more scalable and economically feasible pathways, which is important for wastes conversion. Under these conditions, biomass and biowastes can be more readily converted to produce similar novel carbon materials as observed in vast carbonization articles utilizing HTC at these temperatures.

We investigated the solvothermal carbonization of cellulose in the presence of supercritical $CO_2$ to suggest an alternative to HTC and other pathways for novel carbon material production. Cellulose was chosen as it is not only the most common component of various biomass and biowastes, and significant literature exits on its conversion via various pathways including HTC that can be used for comparison [13,18,24,30,31,53–60]. In addition, cellulose can also act as a more practical alternative feedstock to other carbonization processes such as HTC of monosaccharides such as starch and glucose which also produce carbon microspheres [61,62]. In this paper, supercritical $CO_2$ carbonization (SCC) of cellulose was carried out at moderate temperatures (523 and 623 K) for different residence times that varied between 2 and 5 h. The compositional, morphological, and thermal stability characterization of the filtered residue was further carried out to understand the quality of the product, especially in contrast with carbonized residues from cellulose from other pathways such as HTC and high-temperature pyrolysis. This paper reveals novel information about the conversion of biomass components using supercritical $CO_2$ carbonization, which can establish an efficient and sustainable pathway for waste and biomass utilization as well as novel material synthesis to help support growing bioenergy and biofuels technologies. Conversion at these moderate temperatures and pressures lowers carbon emission while providing easier solids extraction compared with HTC by eliminating filtration requirement and extracting water and pollutants. It also establishes a pathway for $CO_2$ utilization with capability to dispose diverse range of biomass and waste resources including low-grade high moisture content biomass.

## 2 Methods and Materials

Cellulose (called $\alpha$-cellulose) used for the supercritical $CO_2$ carbonization was obtained from Sigma-Aldrich Inc. while $CO_2$ (99.9% pure) was obtained from Airgas. Carbonization tests were carried out in a stainless steel (T316) stirred reactor (having a total volume of 100 ml (Parr 4597 HPHT system)) and had capability to operate up to 773 K temperatures and 34.5 MPa pressures. For each of the test, the reactor chamber was filled with 15 g of cellulose and closed. This reactor was purged using Ar for 5 min to remove the air present, followed by pressurizing with $CO_2$ to an initial pressure of 45 bar. The gas valves were then closed, and the reactor was set to heat to the setpoint temperatures (523 or 623 K). The temperature was monitored which showed the average heating rate to reach these temperatures to be approximately 10.5 K/min and 16 K/min, respectively. We limit this paper to such scenario to avoid any operational parameterization and focus on the feasibility of this process. The setpoint temperature was held constant for residence times of 1, 2, 5, and 8 h for each test case to understand the effect of residence time on the extent of carbonization. The final pressure attained in the reactor was $10 \pm 0.5$ MPa at 523 K and 11.5 MPa at 623 K. After completing the reaction, the reactor was allowed to cool down on its own followed by collection of the solid residue. The residue was then rinsed and filtered using methanol to remove any residual tar/aqueous byproducts followed by drying of the collected char sample. The collected sample was characterized using thermogravimetric analysis (TGA) for thermal stability and proximate analysis, Raman spectroscopy and power X-ray diffraction (XRD) for crystalline content, and scanning electron microscopy (SEM) for morphology.

Thermogravimetric analysis was carried in TA Instruments SDT Q600 wherein for each test, 2–3 mg of the char sample was loaded into alumina pans. The sample was heated to 378 K at 20 K/min followed by staying at that temperature to remove any moisture. This was followed by heating to 12d3 K at 20 K/min. During these steps, 100 sccm of Ar was used as purge gas to measure the volatile content and their evolution temperature. After the reactor reached 1223 K, the purge gas was changed to 100 sccm of dry air and the reactor set to stay at 1223 K for 10 min. The fixed carbon and ash content were then analyzed. This method used was similar to the ASTM standard to obtain standardized proximate analysis [63].

Raman spectroscopy was carried out using 532 nm laser in confocal Raman microscope (Yvon Jobin LabRam ARAMIS) at 10× to obtain averaged sample analysis after calibrating it using silicon standard while multiple low exposure samples were accumulated to obtain sufficient signal-to-noise ratio. XRD analysis was carried out using Bruker D8 Advance powder diffractometer equipped with the sealed tube with Cu anode (X-ray $\lambda = 1.5418$ A), Ni beta-filter, and LynxEye position sensitive detector (3.8 deg window) over angle of diffraction ($2\theta$) of 5–70 deg in step of 0.0211 deg and measuring time of 0.75 s and that resulted in the exposition of 135 s per step. SEM was carried out using Tescan XEIA FEG SEM equipped with Xe Plasma Focused Ion Beam (SEM-FIB) column was used at accelerating voltage of 2 kV to obtain the morphological understanding of the char samples prepared.

## 3 Results and Discussion

The carbonization of cellulose was investigated on various aspects of biomass. Initially, the dried char yields were measured to understand the extent of carbon fixation. After drying, the char

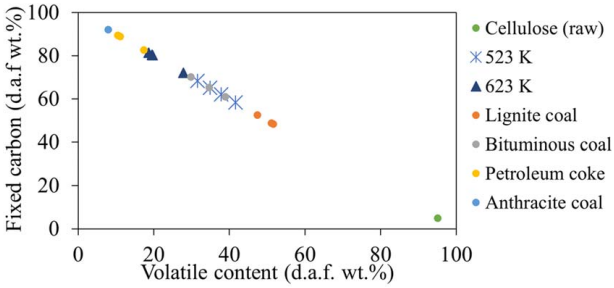


**Fig. 1 Comparison of extents of carbonization from SCC chars with cellulose and different coals (d.a.f: dry ash free) [64]**

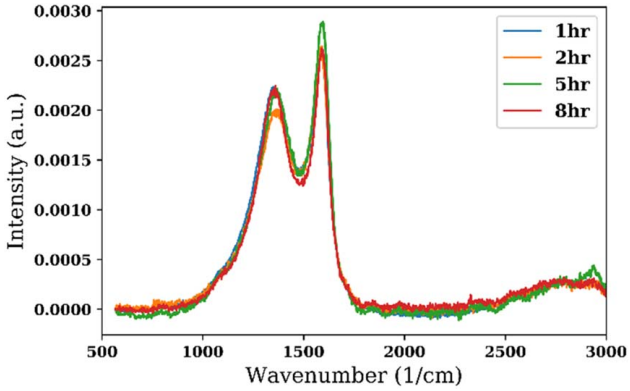


**Fig. 3 Intensity versus wavenumber from Raman spectra of SCC chars obtained at 523 K temperature and different residence times**

yields were found to be 42–45 (wt% of cellulose) at 523 K and 35–40 (wt% of cellulose) at 623 K. While increase in temperature decreased char yields, the influence of residence time on the char yield was found to be minimal and within the extraction error. The decrease in char yield with temperature was due to increased carbonization and further removal of surface oxygenates from the char, which was similar to that observed in HTC of cellulose where the solid yield decreased from 41% to 39% as temperature increased from 548 K to 613 K [30]. Cellulose ($[C_6H_{10}O_5]_n$) contains significant amount of hydroxyl groups which leave during carbonization via dehydration reaction. Maximum theoretical yield from HTC was reported to be 56% at 548 K and 45% at 613 K assuming the byproducts to be only $H_2O$ and $CO_2$ from dehydration and decarboxylation [6,7]. This reveals that supercritical $CO_2$-assisted carbonization can also produce carbonization close to theoretical limits suggesting its high carbon fixing efficiency that can replace HTC. To further analyze the extent of carbonization and the stability of chars obtained, TGA studies were carried out.

**3.1 Thermogravimetric Analysis of Char Residues.** Thermogravimetric analysis was utilized to understand the thermal decomposition behavior of the chars obtained along with their proximate analysis for the carbonization level. This was compared with various ranks of coals to assess the quality of chars and the potential of this process in carbon sequestration as well as applicability limits of the chars in catalytic reactions.

*3.1.1 Carbon Fixation.* Proximate analysis of the chars was obtained by analyzing the TGA data for the method mentioned. Based on these analyses, the comparison of volatile content versus fixed carbon content is plotted in Fig. 1 for the chars obtained from supercritical $CO_2$ carbonization of cellulose in comparison with pure cellulose feedstock utilized for these tests. The results from different ranks of coal are also included in Fig. 1 [64]. The volatiles content significantly reduced from 95% in cellulose to 31–41% for SCC chars obtained at 523 K and only 18–27% from those at 623 K. This meant an increase in fixed carbon content via carbonization from 5% in cellulose to 58–65% for chars from 523 K and 72–81% for chars from 623 K. An increase in fixed carbon content is a resultant of improved extent of carbonization which increased with temperature as more volatiles evolved during pyrolysis and rearranged as char. Comparison with different ranks of coal reveals that SCC chars from 523 K were similar to bituminous coals while those from 623 K had better fixed carbon content than bituminous coals to reach as high as petroleum coke. This reveals the carbonization capability of SCC at moderate reactor conditions to improve the quality of the feedstock. While this has been investigated on cellulose, it can be potentially used for other low-grade feedstocks to improve their quality in terms of fixed carbon content which can allow for improved energy density and transportability to effectively improve their value.

While the volatiles and fixed carbon content in the chars varied with residence times, a discernable trend was difficult to observe, possibly due to irregularities in process performance arising from the use of gaseous $CO_2$ as the precursor to reach supercritical $CO_2$. With the initial pressure used in these experiments, the transition point of $CO_2$ gas to supercritical phase occurred at a higher temperature, possibly when the decomposition of cellulose had already started. The focus of this paper has been limited to establishing the feasibility of SCC to match HTC and other carbonization pathways to obtain valuable carbon. The challenges of reaction control and its impact on carbonization will be investigated in one of our future studies.

*3.1.2 Thermal Stability.* To understand the thermal stability of the chars obtained, the normalized mass-loss derivatives were calculated from the TGA data and compared with cellulose characteristics, see Fig. 2. In this figure, $\alpha$ is the normalized mass-loss

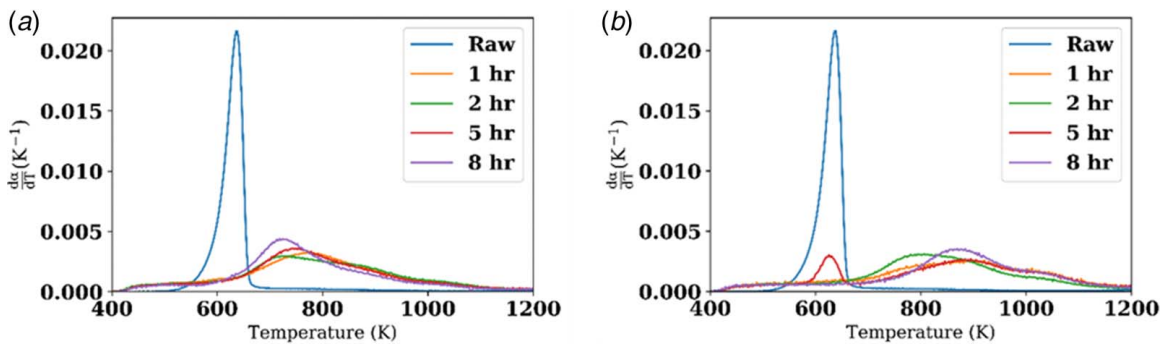


**Fig. 2 TG behavior of SCC chars obtained at (*a*) 523 K and (*b*) 623 K temperatures and different residence times (and also raw cellulose)**

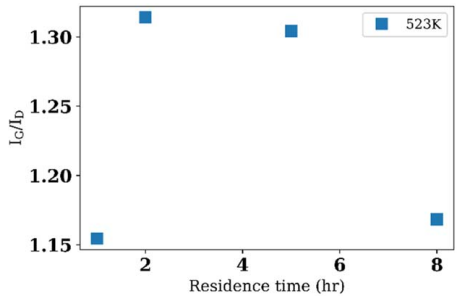


**Fig. 4 Degree of graphitization indicated from Raman spectra of SCC-char samples at 523 K and different residence times**

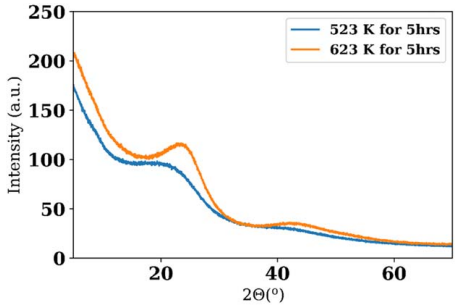


**Fig. 5 Powder XRD patterns of selected char samples obtained from SCC of cellulose at 523 and 623 K temperature at 5 h residence time**

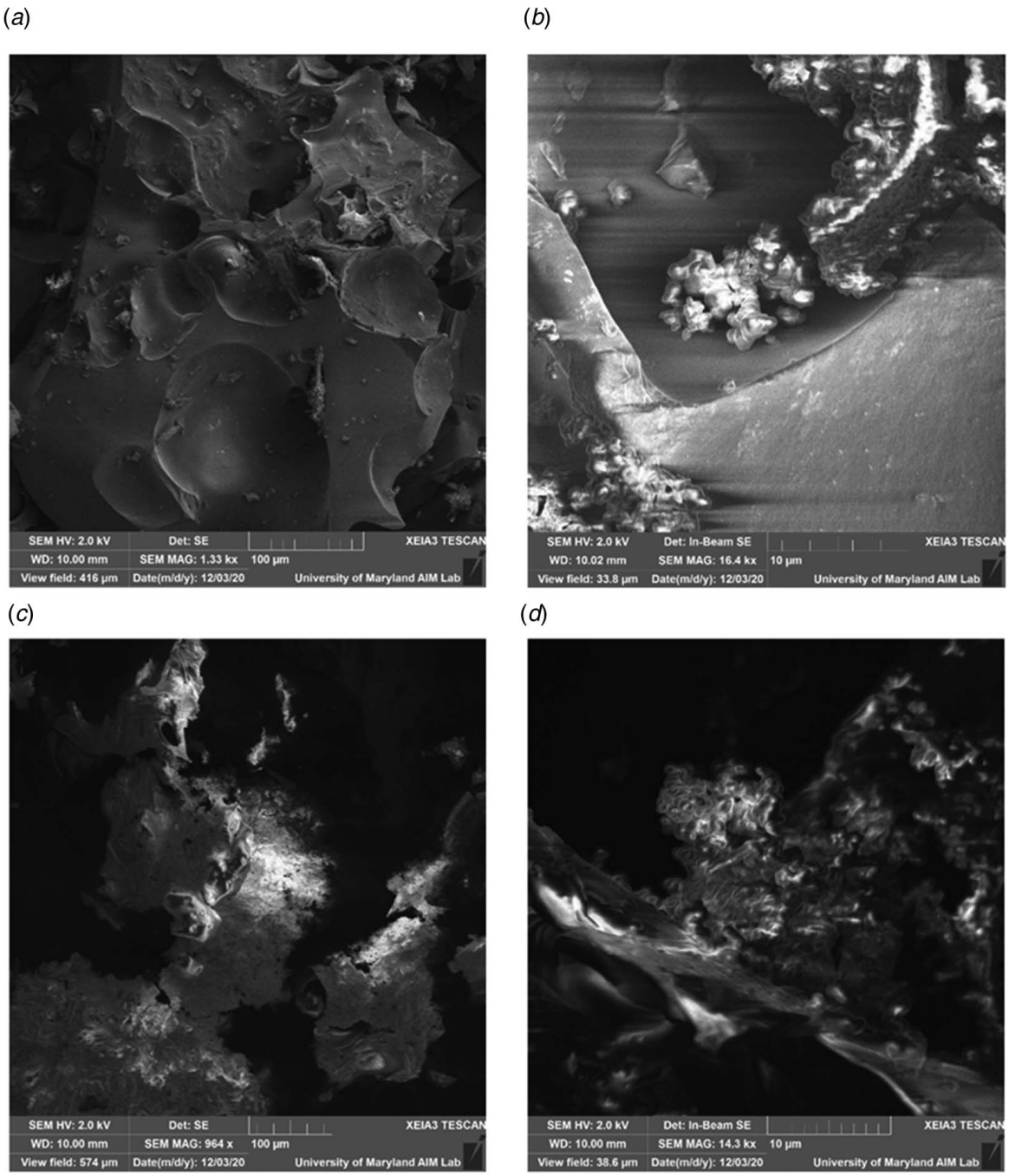


**Fig. 6 SEM images of the chars obtained from SCC of cellulose at (*a*) 523 K for 2 h of residence time, (*b*) 523 K for 2 h (magnified), (c) 523 K for 5 h of residence time, and (*d*) 523 K for 5 h (magnified)**

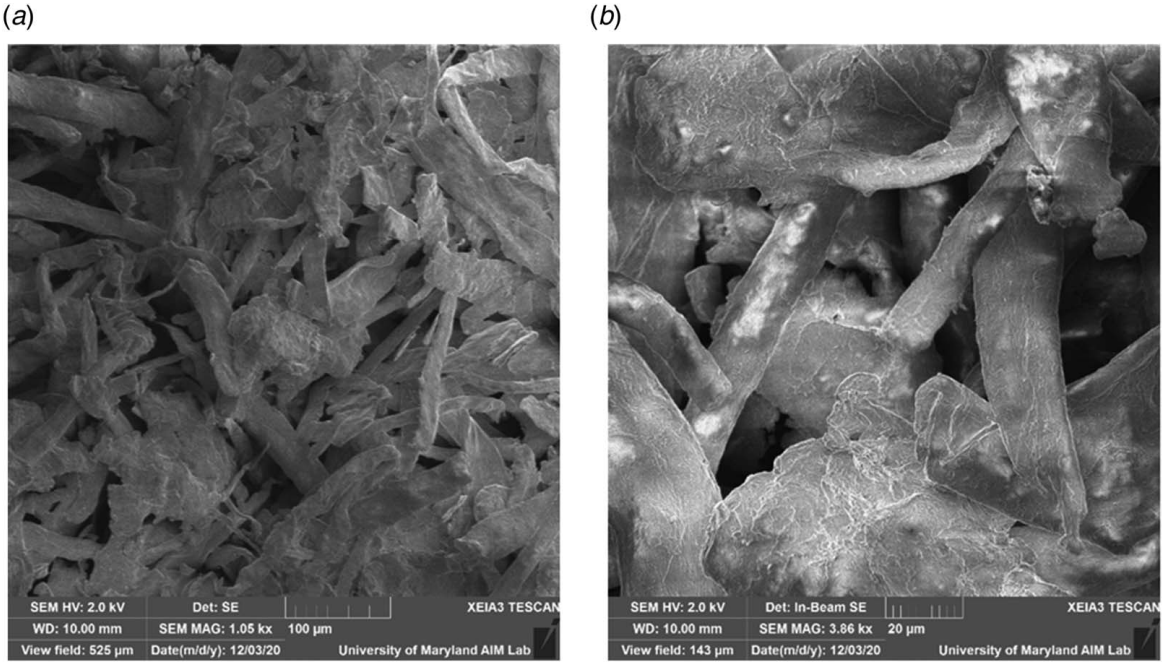


**Fig. 7 SEM images of (*a*) the raw cellulose and (*b*) raw cellulose (magnified) used for the SCC tests**

$(\alpha(T) = (m_o - m_T)/(m_o - m_f))$ where $m_o$ and $m_f$ are the initial and final mass of the sample in the TGA while $m_T$ is the mass recorded at any intermediate temperature $T$ and "Raw" refers to pure cellulose sample.

Figure 2(*a*) reveals that pyrolysis of cellulose occurs between 520 and 680 K while the peaking at 636 K. So, both the SCC temperatures examined in this paper were within the pyrolytic temperature range of cellulose but below its peak value, suggesting that moderate temperature operation can be utilized via SCC to carbonize cellulose. It also reveals that char samples decompose over a broader temperature range while peaking at approximately 720 K. This broad temperature distribution in pyrolysis of SCC chars could arise from rearrangement reactions within the char and cracking of its aliphatic content to form increased aromatic carbon while releasing $H_2$, $CO_2$, and $H_2O$. Figure 2(*b*) reveals that for chars obtained at 623 K, the decomposition peak increased to 800–900 K. This also suggests higher thermal stability of the chars obtained from SCC compared with chars obtained from slow-pyrolysis and is attributed to its improved thermal stability via low-temperature processing. A small peak aligning with cellulose is also observed in Fig. 2(*b*), possibly from the irregular operation of the current pathway to reach supercritical $CO_2$ leading to some uncarbonized cellulosic content. The impact of residence time seems to be irregular but it is minimal. Char yield close to the theoretical value and improved thermal stability and fixed carbon content suggests improved value via SCC in terms of carbon sequestration and decreased carbon emission, similar to HTC. Note that SCC avoided water treatment and other environmental compatibility and process viability issues present in HTC [6].

**3.2 Crystalline Content and Composition of Char Residues.** To characterize the chars in terms of their crystalline and amorphous carbon and understand its composition, Raman spectroscopy and powder XRD were carried out. Figure 3 reveals the processed normalized spectra of chars obtained from different SCC residence times. It shows broadband intensity ($I_D$) behavior of D-band (1360 $cm^{-1}$) and intensity ($I_G$) behavior of G-band (1580 $cm^{-1}$), which were also observed to overlap in the char samples [65–68]. D-band corresponds to the $sp^3$ hybridized carbon which is present in char in the form of linking chains, surface functional groups while G-band represents uniform aromatic rings and graphitic crystallites. The presence of G-band suggests the formation of aromatic crystallites similar to graphene layers, which are incorporated in an amorphous carbon matrix via $sp^3$ carbon links from the D-band. Although G-band represents the formation of crystallite structures in the char matrix, the broadband behavior of the D-band and the significant overlap between these bands represent significantly amorphous carbon. The ratio of $I_G/I_D$ represents the degree of graphitization from the aromatic crystallite structures present in the chain char. This was similar to the char obtained via HTC of cellulose [30].

The ratio of the peak intensities, i.e., $I_G/I_D$ was utilized in the literature to understand the degree of graphitization in a carbonized sample with motivation from such comparison with pure graphite and graphite sample with defects [13,65,66]. Figure 4 shows the $I_G/I_D$ of the SCC-char samples that helps to understand the role of residence time on the degree of graphitization. An increase in temperature increased the ratio ($I_G/I_D$) as carbonization at higher temperatures leads to increased order in the crystallite formation and decreased the aliphatic carbon bonds that correspond to D-band. Figure 4 also suggests the presence of a peak in the ratios with respect to increase in residence time. Among the tested values, at 523 K, yield in value of $I_G/I_D$ was 1.31 at 2 h and ~1.3 at 5 h. This suggests that a time duration of 2–5 h is favorable for char graphitization. While the range of this ratio is higher than bituminous coals, activated carbon, and other suggested carbonized samples used for graphene extraction in the literature, it is similar to that of cellulose char from HTC [10,69–71]. Typically, higher the ratio, more the order in carbonized samples. Further examination is necessary to understand such a behavior of decreasing ratio with increase/decrease in residence time as the correlation between $I_G/I_D$ values and the order of graphitic samples is quasi-linear. This relation gets complicated from samples with significant disorder, such as our samples and thus limiting the scope of Raman spectroscopy [66]. In order to further understand the impact of residence time on the char matrix, powder XRD was carried out.

Figure 5 shows the XRD patterns against angle of diffraction ($2\theta$) of high residence time SCC-char samples obtained at 523 K and 623 K at 5 h of residence time. The results reveal that while the char samples are mostly amorphous, an increase in peak value at 23 deg and ~46 deg was observed at high temperature which

correspond to (002) and (100) crystal planes of graphitic layers in amorphous carbon in the char samples [8,49,59,72]. They can be mildly seen at 523 K that shows a small increase at 20 deg. This suggests the growth of graphitic components while the broadband behavior of these peaks suggests the char to be mostly amorphous. An increase in the (002) peak height was also observed with decrease in residence time to support the lowering of $I_G/I_D$ with increase in residence time. Further investigations into this observed decrease in graphitization are necessary to understand this behavior. The comparably high $I_G/I_D$ and significant presence of amorphous graphite peaks suggests the presence of a significant number of disorderly arranged local crystallite portions in the char matrix. These patterns are similar to high-ranking coals such as carbonized bituminous coals which suggest that these SCC chars can be utilized to support the material needs. They are currently addressed using coals such as graphene and graphene quantum dots extraction which can be obtained by further processing these chars to recover the graphene dots from the matrix which are high-value carbon products with novel and diverse applications [10].

**3.3 Morphology of the Char Residues.** The morphology of the filtered and dried char samples was obtained via SEM to understand the type of carbon structures and the porosity attained using SCC of cellulose.

Figure 6 shows the morphology of chars obtained at 523 K at 2 and 5 h of residence time. The results reveal the presence of linked chains of carbon microspheres as seen in the magnified

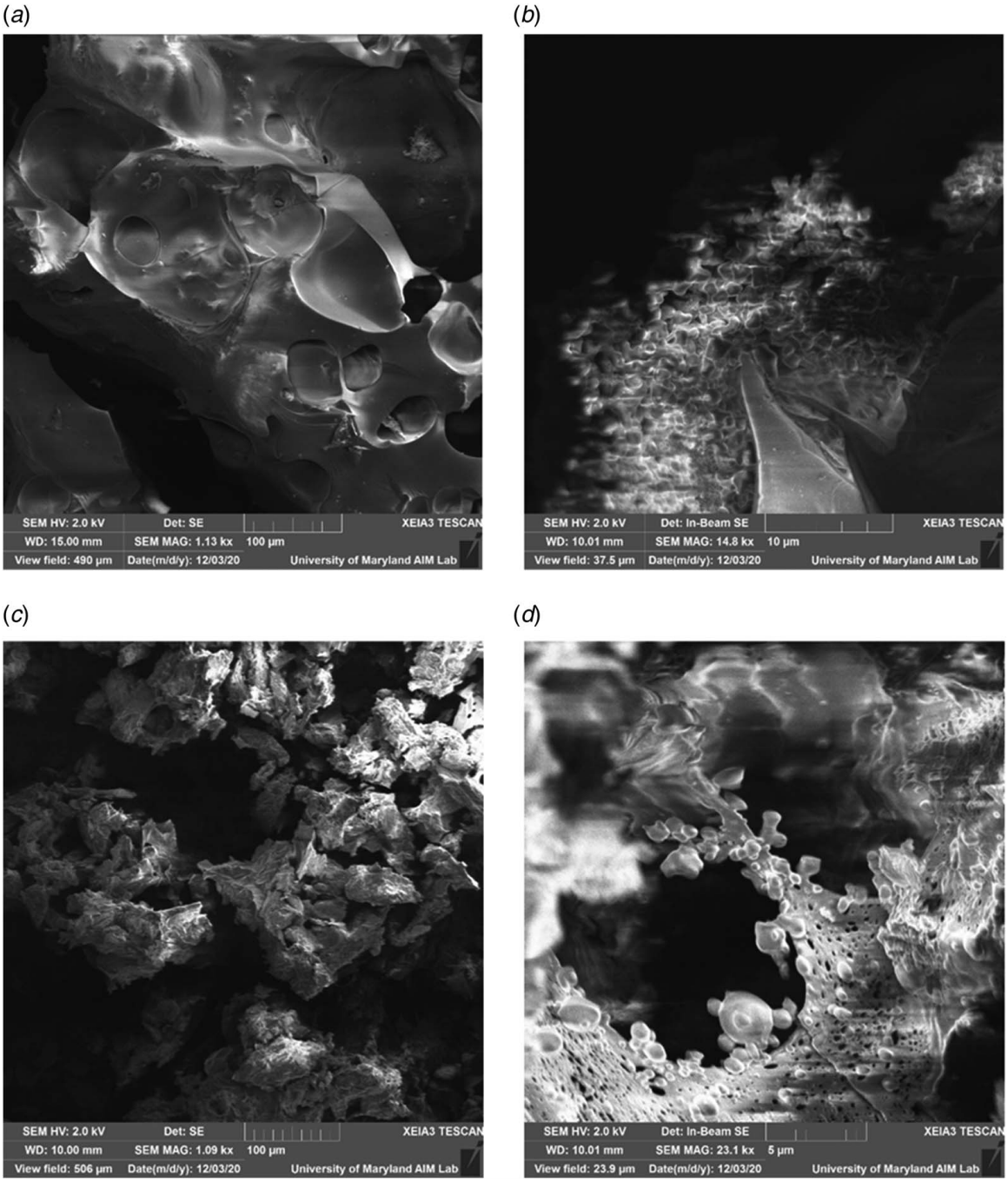


**Fig. 8 SEM images of the chars obtained from SCC of cellulose at (*a*) 623 K for 2 h of residence time, (*b*) 623 K for 2 h (magnified), (c) 623 K for 5 h of residence time, and (*d*) 623 K for 5 h (magnified)**

images. Other disordered particles were also formed while the surface was found to be of low porosity, similar to that from hydrochars [29,30,32]. While an increase in residence times at this temperature resulted in rougher surfaces, the separation of the carbon microspheres can also be seen. Figure 6(*d*) reveals the presence of some partially separated carbon microspheres. The size of these spheres did not seem to change with residence times. Based on the observation from these images, the size of linkages and the microspheres was found to be around 1 $\mu$m or less in contrast with the initial morphology of raw cellulose which was composed of microfibers of at least 20 $\mu$m diameter, see Fig. 7. This size is smaller than that observed from HTC of cellulose (2–10 $\mu$m) which also revealed this to decrease with increase in feedstock loading with respect to water while also making it more disordered. The uniformity in these carbon microspheres in SCC chars lies in their characteristic size. However, the shape is relatively less uniform compared with those from HTC. This could be from the early onset of cellulose conversion before the $CO_2$ reaches supercritical phase leading to non-uniformity, a limitation of the current setup which the authors intend to investigate report in their future investigations.

Figure 8 shows the relative impact of temperature which reveals the morphology of SCC chars obtained at 623 K for two different residence times. It is to be noted that the magnification was varied for each image to obtain the objects of interest as some morphological patterns varied in size. An increase in temperature seems to clearly increase the surface area as seen from Fig. 8(*b*), which shows a conglomerate of small carbon particles which are possibly linked. At this temperature, as the residence time increased, the microspheres separated while at 5 h, this seems to form non-uniform clusters of larger size which are conjectured to be correlated with the decrease in the degree of graphitization. Further investigations (beyond the scope of this paper) are needed to understand this behavior. Nevertheless, one can clearly see the increase in porosity and separation of the particles with increase in time from 2 to 5 h. Figure 8(*d*) shows the partially separate cluster of carbon microspheres along with pores of size less than 1 $\mu$m on the connecting surface. This suggests that long residence time of 5 h at 623 K is favorable to obtain improved graphitic content along with morphology containing carbon microspheres and surface with higher porosity.

Parametric investigations into the impact of individual operating conditions such as temperature, loading, residence time, feedstock size, and other parameters are planned to be carried out in our future investigations to improve the quality of the SCC chars obtained followed by examining the capabilities of these chars in diverse lab-scale applications such as activated carbon, graphene, graphene quantum dot synthesis, electrochemical and thermal catalysis, anode material in Li-ion batteries, and other novel carbon material applications.

## 4 Conclusions

This paper establishes the capability of SCC of cellulose as a viable pathway to obtain high-value carbon products and precursors which can improve the viability of biomass and biowastes utilization for sustainable material production in addition to energy use. Supercritical $CO_2$ provides a better alternative to water and thus SCC to HTC for carbon fixation as it eliminates the water cleaning requirements from carcinogenic byproducts before their disposal. This then provides regenerative capability and easier recovery of byproducts and potentially eliminating the need for drying of wet wastes and the final carbon residue. SCC of cellulose at 523 K and 623 K for 2 and 5 h showed char yields of 42–35% that decreased with temperature with significantly high fixed carbon content (60–80% that increased with temperature). These values represent good similarity to those with bituminous coal and petroleum coke. Devolatilization of these chars was observed at 720 K for SCC at 523 K and 800–900 K for SCC at 623 K along with broadband behavior suggesting improving thermal stability of the chars with SCC temperature. Raman spectroscopy of these chars revealed the presence of aliphatic linked carbons connecting different local graphitic crystallites. An increase in temperature increased the graphitic content while an increase in residence time provided a peak in graphitization at 5 h for 623 K. This was supported by the powder XRD patterns of these chars. The morphological investigation of these chars using SEM revealed the presence of clusters of carbon microspheres which separated with increase in residence time. An increase in SCC temperature provided chars with more porosity while also simultaneously improved the microsphere content. These results establish that the chars obtained from SCC of cellulose to be of comparable quality to high-ranking coals. They offer additional advantages over HTC while being sustainable and carbon neutral compared with fossil-fuels. This makes SCC of biomass and biowastes as a novel alternative carbonization pathway which not only converts low-grade carbon-neutral feedstocks into valuable carbon but also provides a utility for supercritical $CO_2$ with lowered carbon emissions compared with any other carbonization pathway.


## Acknowledgment

This research was supported by Office of Naval Research (ONR), and their support is gratefully acknowledged. Kiran G. Burra was supported by Ann G. Wylie fellowship and Hulka Energy fellowship which is gratefully acknowledged. The support provided by the Maryland NanoCenter and its AIMLab and Surface Analysis Center in acquiring SEM and Raman spectra is gratefully acknowledged. The support of University of Maryland, X-ray Crystallographic Center, and Dr. Peter Y. Zavalij in obtaining XRD is also gratefully acknowledged.


## Conflict of Interest

There are no conflicts of interest.

## References


[1] EPA, 2019, "Advancing Sustainable Materials Management: Facts and Figures Report," United States Environmental Protection Agency, https://www.epa.gov/sites/production/files/2021-01/documents/2018_ff_fact_sheet_dec_2020_fnl_508.pdf

[2] Burra, K. G., and Gupta, A. K., 2018, "Thermochemical Reforming of Wastes to Renewable Fuels," *Energy for Propulsion: A Sustainable Technologies Approach*, A. K. Runchal, A. K. Gupta, A. Kushari, A. De, and S. K. Aggarwal, eds., Springer, Singapore, pp. 395–428.

[3] Olah, G. A., Prakash, G. K. S., and Goeppert, A., 2011, "Anthropogenic Chemical Carbon Cycle for a Sustainable Future," J. Am. Chem. Soc., **133**(33), pp. 12881–12898.

[4] Zhang, H., Cheng, Y.-T., Vispute, T. P., Xiao, R., and Huber, G. W., 2011, "Catalytic Conversion of Biomass-Derived Feedstocks Into Olefins and Aromatics With ZSM-5: The Hydrogen to Carbon Effective Ratio," Energy Environ. Sci., **4**(6), pp. 2297–2307.

[5] Demirbas, A., 2004, "Pyrolysis of Municipal Plastic Wastes for Recovery of Gasoline-Range Hydrocarbons," J. Anal. Appl. Pyrolysis, **72**(1), pp. 97–102.

[6] Libra, J. A., Ro, K. S., Kammann, C., Funke, A., Berge, N. D., Neubauer, Y., Titirici, M.-M., Fühner, C., Bens, O., Kern, J., and Emmerich, K.-H., 2011, "Hydrothermal Carbonization of Biomass Residuals: A Comparative Review of the Chemistry, Processes and Applications of Wet and Dry Pyrolysis," Biofuels, **2**(1), pp. 71–106.

[7] Titirici, M.-M., and Antonietti, M., 2010, "Chemistry and Materials Options of Sustainable Carbon Materials Made by Hydrothermal Carbonization," Chem. Soc. Rev., **39**(1), pp. 103–116.

[8] Jung, S. H., Myung, Y., Kim, B. N., Kim, I. G., You, I. K., and Kim, T. Y., 2018, "Activated Biomass-Derived Graphene-Based Carbons for Supercapacitors With High Energy and Power Density," Sci. Rep., **8**, pp. 1–8.

[9] Xing, B., Zhang, C., Cao, Y., Huang, G., Liu, Q., Zhang, C., Chen, Z., Yi, G., Chen, L., and Yu, J., 2018, "Preparation of Synthetic Graphite From Bituminous Coal as Anode Materials for High Performance Lithium-Ion Batteries," Fuel Process. Technol., **172**, pp. 162–171.

[10] Saikia, M., Das, T., Dihingia, N., Fan, X., Silva, L. F. O., and Saikia, B. K., 2020, "Formation of Carbon Quantum Dots and Graphene Nanosheets From Different Abundant Carbonaceous Materials," Diamond Relat. Mater., **106**, p. 107813.

[11] Liu, P., Si, Z., Lv, W., Wu, X., Ran, R., Weng, D., and Kang, F., 2019, "Synthesizing Multilayer Graphene From Amorphous Activated Carbon via Ammonia-Assisted Hydrothermal Method," Carbon, **152**, pp. 24–32.
[12] Li, S., Li, F., Wang, J., Tian, L., Zhang, H., and Zhang, S., 2018, "Preparation of Hierarchically Porous Graphitic Carbon Spheres and Their Applications in Supercapacitors and Dye Adsorption," Nanomaterials, **8**(8), p. 625.
[13] Chen, C., Sun, K., Wang, A., Wang, S., and Jiang, J., 2018, "Catalytic Graphitization of Cellulose Using Nickel as Catalyst," Bioresources, **13**, pp. 3165–3176.
[14] Bazargan, A., Yan, Y., Hui, C. W., and McKay, G., 2013, "A Review: Synthesis of Carbon-Based Nano and Micro Materials by High Temperature and High Pressure," Ind. Eng. Chem. Res., **52**(36), pp. 12689–12702.
[15] Goto, M., 2009, "Chemical Recycling of Plastics Using Sub- and Supercritical Fluids," J. Supercrit. Fluids, **47**(3), pp. 500–507.
[16] Inagaki, M., Park, K. C., and Endo, M., 2010, "Carbonization Under Pressure," Xinxing Tan Cailiao/New Carbon Mater., **25**(6), pp. 409–420.
[17] Jain, A. A., Mehra, A., and Ranade V, V., 2016, "Processing of TGA Data: Analysis of Isoconversional and Model Fitting Methods," Fuel, **165**, pp. 490–498.
[18] Simsir, H., Eltugral, N., and Karagoz, S., 2017, "Hydrothermal Carbonization for the Preparation of Hydrochars From Glucose, Cellulose, Chitin, Chitosan and Wood Chips via Low-Temperature and Their Characterization," Bioresour. Technol., **246**, pp. 82–87.
[19] Berge, N. D., Ro, K. S., Mao, J., Flora, J. R. V., Chappell, M. A., and Bae, S., 2011, "Hydrothermal Carbonization of Municipal Waste Streams," Environ. Sci. Technol., **45**(13), pp. 5696–5703.
[20] Saqib, N. U., Sharma, H. B., Baroutian, S., Dubey, B., and Sarmah, A. K., 2019, "Valorisation of Food Waste via Hydrothermal Carbonisation and Techno-Economic Feasibility Assessment," Sci. Total Environ., **690**, pp. 261–276.
[21] Maniscalco, M. P., Volpe, M., and Messineo, A., 2020, "Hydrothermal Carbonization as a Valuable Tool for Energy and Environmental Applications: A Review," Energies, **13**(16), p. 4098.
[22] Bevan, E., Fu, J., and Zheng, Y., 2020, "Challenges and Opportunities of Hydrothermal Carbonisation in the UK; Case Study in Chirnside," RSC Adv., **10**(52), pp. 31586–31610.
[23] Pawlak-Kruczek, H., Urbanowska, A., Yang, W., Brem, G., Magdziarz, A., Seruga, P., Niedzwiecki, L., Pozarlik, A., Mlonka-Mędrala, A., Kabsch-Korbutowicz, M., Bramer, E., Baranowski, M., Sieradzka, M., and Tkaczuk-Serafin, M., 2020, "Industrial Process Description for the Recovery of Agricultural Water From Digestate," ASME J. Energy Resour. Technol., **142**(7), p. 070917.
[24] Faradilla, R. F., Lucia, L., and Hakovirta, M., 2020, "Remarkable Physical and Thermal Properties of Hydrothermal Carbonized Nanoscale Cellulose Observed From Citric Acid Catalysis and Acetone Rinsing," Nanomaterials, **10**(6), pp. 1–13.
[25] Susanti, R. F., Arie, A. A., Kristianto, H., Erico, M., Kevin, G., and Devianto, H., 2019, "Activated Carbon From Citric Acid Catalyzed Hydrothermal Carbonization and Chemical Activation of Salacca Peel as Potential Electrode for Lithium Ion Capacitor's Cathode," Ionics, **25**(8), pp. 3915–3925.
[26] Nizamuddin, S., Baloch, H. A., Griffin, G. J., Mubarak, N. M., Bhutto, A. W., Abro, R., Mazari, S. A., and Ali, B. S., 2017, "An Overview of Effect of Process Parameters on Hydrothermal Carbonization of Biomass," Renew. Sustain. Energy Rev., **73**, pp. 1289–1299.
[27] Falco, C., Perez Caballero, F., Babonneau, F., Gervais, C., Laurent, G., Titirici, M. M., and Baccile, N., 2011, "Hydrothermal Carbon From Biomass: Structural Differences Between Hydrothermal and Pyrolyzed Carbons via 13C Solid State NMR," Langmuir, **27**(23), pp. 14460–14471.
[28] He, C., Giannis, A., and Wang, J.-Y., 2013, "Conversion of Sewage Sludge to Clean Solid Fuel Using Hydrothermal Carbonization: Hydrochar Fuel Characteristics and Combustion Behavior," Appl. Energy, **111**, pp. 257–266.
[29] Sevilla, M., Maciá-Agulló, J. A., and Fuertes, A. B., 2011, "Hydrothermal Carbonization of Biomass as a Route for the Sequestration of $CO_2$: Chemical and Structural Properties of the Carbonized Products," Biomass Bioenergy, **35**(7), pp. 3152–3159.
[30] Sevilla, M., and Fuertes, A. B., 2009, "The Production of Carbon Materials by Hydrothermal Carbonization of Cellulose," Carbon, **47**(9), pp. 2281–2289.
[31] Sheng, K., Zhang, S., Liu, J., Shuang, E., Jin, C., and Xu, Z., 2019, "Hydrothermal Carbonization of Cellulose and Xylan Into Hydrochars and Application on Glucose Isomerization," J. Cleaner Prod., **237**, p. 117831.
[32] Guiotoku, M., Hansel, F. A., Novotny, E. H., and de Freitas Maia, C. M. B., 2012, "Molecular and Morphological Characterization of Hydrochar Produced by Microwave-Assisted Hydrothermal Carbonization of Cellulose," Pesqui. Agropecu. Bras., **47**(5), pp. 687–692.
[33] Higgins, L. J. R., Brown, A. P., Harrington, J. P., Ross, A. B., Kaulich, B., and Mishra, B., 2020, "Evidence for a Core-Shell Structure of Hydrothermal Carbon," Carbon, **161**, pp. 423–431.
[34] Kambo, H. S., and Dutta, A., 2015, "A Comparative Review of Biochar and Hydrochar in Terms of Production, Physico-Chemical Properties and Applications," Renew. Sustain. Energy Rev., **45**, pp. 359–378.
[35] Zhang, X., Heinonen, S., and Levänen, E., 2014, "Applications of Supercritical Carbon Dioxide in Materials Processing and Synthesis," RSC Adv., **4**(105), pp. 61137–61152.
[36] Sanli, D., Bozbag, S. E., and Erkey, C., 2012, "Synthesis of Nanostructured Materials Using Supercritical $CO_2$: Part I. Physical Transformations," J. Mater. Sci., **47**(7), pp. 2995–3025.
[37] Kalina, J., Skorek-Osikowska, A., Bartela, Ł, Gładysz, P., and Lampert, K., 2020, "Evaluation of Technological Options for Carbon Dioxide Utilization," ASME J. Energy Resour. Technol., **142**(9), p. 090901.
[38] Strakey, P. A., 2019, "Oxy-Combustion Modeling for Direct-Fired Supercritical $CO_2$ Power Cycles," ASME J. Energy Resour. Technol., **141**(7), p. 070706.
[39] Hoffman, B. T., and Shoaib, S., 2014, "$CO_2$ Flooding to Increase Recovery for Unconventional Liquids-Rich Reservoirs," ASME J. Energy Resour. Technol., **136**(2), p. 022801.
[40] Jessop, P. G., and Leitner, W., 1999, *Chemical Synthesis Using Supercritical Fluids*, Wiley-VCH Verlag, Weinheim, Germany.
[41] Long, T. E., Voit, B., and Okay, O., 2015, *Porous Carbons—Hyperbranched Polymers—Polymer Solvation*, Vol. 266. Springer-Verlag, Berlin/Heidelberg.
[42] Gong, J., Zhao, G., Wang, G., Zhang, L., and Li, B., 2019, "Fabrication of Macroporous Carbon Monoliths With Controllable Structure via Supercritical $CO_2$ Foaming of Polyacrylonitrile," J. $CO_2$ Util., **33**, pp. 330–340.
[43] Cooper, A. I., 2001, "Recent Developments in Materials Synthesis and Processing Using Supercritical $CO_2$," Adv. Mater., **13**(14), pp. 1111–1114.
[44] Li, L., Zheng, X., Wang, J., Sun, Q., and Xu, Q., 2013, "Solvent-Exfoliated and Functionalized Graphene With Assistance of Supercritical Carbon Dioxide," ACS Sustain. Chem. Eng., **1**(1), pp. 144–151.
[45] Gao, H., Xue, C., Hu, G., and Zhu, K., 2017, "Production of Graphene Quantum Dots by Ultrasound-Assisted Exfoliation in Supercritical $CO_2$/$H_2O$ Medium," Ultrason. Sonochem., **37**, pp. 120–127.
[46] Li, H., Chang, Q., Dai, Z., Chen, X., Yu, G., and Wang, F., 2017, "Upgrading Effects of Supercritical Carbon Dioxide Extraction on Physicochemical Characteristics of Chinese Low-Rank Coals," Energy Fuels, **31**(12), pp. 13305–13316.
[47] Putrino, F. M., Tedesco, M., Bodini, R. B., and de Oliveira, A. L., 2020, "Study of Supercritical Carbon Dioxide Pretreatment Processes on Green Coconut Fiber to Enhance Enzymatic Hydrolysis of Cellulose," Bioresour. Technol., **309**, p. 123387.
[48] Kim, K. H., and Hong, J., 2001, "Supercritical $CO_2$ Pretreatment of Lignocellulose Enhances Enzymatic Cellulose Hydrolysis," Bioresour. Technol., **77**(2), pp. 139–144.
[49] Wei, L., Yan, N., and Chen, Q., 2011, "Converting Poly(Ethylene Terephthalate) Waste Into Carbon Microspheres in a Supercritical $CO_2$ System," Environ. Sci. Technol., **45**(2), pp. 534–539.
[50] Pol, V. G., Pol, S. V., Calderon Moreno, J. M., and Gedanken, A., 2006, "High Yield One-Step Synthesis of Carbon Spheres Produced by Dissociating Individual Hydrocarbons at Their Autogenic Pressure at Low Temperatures," Carbon, **44**(15), pp. 3285–3292.
[51] Yu, B., Kong, X., Wei, L., and Chen, Q., 2011, "Treatment of Discarded Oil in Supercritical Carbon Dioxide for Preparation of Carbon Microspheres," J. Mater. Cycles Waste Manag., **13**(4), pp. 298–304.
[52] Romero-Anaya, A. J., Ouzzine, M., Lillo-Ródenas, M. A., and Linares-Solano, A., 2014, "Spherical Carbons: Synthesis, Characterization and Activation Processes," Carbon, **68**, pp. 296–307.
[53] Álvarez-Murillo, A., Sabio, E., Ledesma, B., Román, S., and González-García, C. M., 2016, "Generation of Biofuel From Hydrothermal Carbonization of Cellulose. Kinetics Modelling," Energy, **94**, pp. 600–608.
[54] Volpe, M., Messineo, A., Mäkelä, M., Barr, M. R., Volpe, R., Corrado, C., and Fiori, L., 2020, "Reactivity of Cellulose During Hydrothermal Carbonization of Lignocellulosic Biomass," Fuel. Process. Technol., **206**, p. 106456.
[55] Gao, Y., Wang, X., Yang, H., and Chen, H., 2012, "Characterization of Products From Hydrothermal Treatments of Cellulose," Energy, **42**(1), pp. 457–465.
[56] Cardea, S., and De Marco, I., 2020, "Cellulose Acetate and Supercritical Carbon Dioxide: Membranes, Nanoparticles, Microparticles and Nanostructured Filaments," Polymers, **12**(1), p. 162.
[57] Johnson, S., Faradilla, R. F., Venditti, R. A., Lucia, L., and Hakovirta, M., 2020, "Hydrothermal Carbonization of Nanofibrillated Cellulose: A Pioneering Model Study Demonstrating the Effect of Size on Final Material Qualities," ACS Sustain. Chem. Eng., **8**(4), pp. 1823–1830.
[58] Falco, C., Baccile, N., and Titirici, M. M., 2011, "Morphological and Structural Differences Between Glucose, Cellulose and Lignocellulosic Biomass Derived Hydrothermal Carbons," Green Chem., **13**(11), pp. 3273–3281.
[59] García-Bordejé, E., Pires, E., and Fraile, J. M., 2017, "Parametric Study of the Hydrothermal Carbonization of Cellulose and Effect of Acidic Conditions," Carbon, **123**, pp. 421–432.
[60] Yang, G., Jiang, Y., Yang, X., Xu, Y., Miao, S., and Li, F., 2017, "The Interaction of Cellulose and Montmorillonite in a Hydrothermal Process," J. Sol-Gel Sci. Technol., **82**(3), pp. 846–854.
[61] Roldán, L., Santos, I., Armenise, S., Fraile, J. M., and García-Bordejé, E., 2012, "The Formation of a Hydrothermal Carbon Coating on Graphite Microfiber Felts for Using as Structured Acid Catalyst," Carbon, **50**, pp. 1363–1372.
[62] Liang, J., Liu, Y., and Zhang, J., 2011, "Effect of Solution pH on the Carbon Microsphere Synthesized by Hydrothermal Carbonization," Procedia Environ. Sci., **11**, pp. 1322–1327.
[63] 2015, Standard Test Methods for Proximate Analysis of Coal and Coke by Macro Thermogravimetric Analysis 1.
[64] Phyllis2, Database for Biomass and Waste. Energy Res Cent Netherlands 2018. https://www.ecn.nl/phyllis2/Biomass/View/3501, Accessed May 28, 2018.
[65] Jorio, A., Ferreira, E. H. M., Moutinho, M. V. O., Stavale, F., Achete, C. A., and Capaz, R. B., 2010, "Measuring Disorder in Graphene With the G and D Bands," Phys. Status Solidi B, **247**(11–12), pp. 2980–2982.
[66] Quirico, E., Rouzaud, J. N., Bonal, L., and Montagnac, G., 2005, "Maturation Grade of Coals as Revealed by Raman Spectroscopy: Progress and Problems," Spectrochim. Acta, Part A, **61**(10), pp. 2368–2377.
[67] Franklin, R. E., 1951, "Crystallite Growth in Graphitizing and Non-Graphitizing Carbons," Proc. R. Soc. A, **209**, pp. 196–218.

[68] Zhang, H., Zhang, F., and Huang, Q., 2017, "Highly Effective Removal of Malachite Green From Aqueous Solution by Hydrochar Derived From Phycocyanin-Extracted Algal Bloom Residues Through Hydrothermal Carbonization," RSC Adv., **7**(10), pp. 5790–5799.
[69] Das, T., Boruah, P. K., Das, M. R., and Saikia, B. K., 2016, "Formation of Onion-Like Fullerene and Chemically Converted Graphene-Like Nanosheets From Low-Quality Coals: Application in Photocatalytic Degradation of 2-Nitrophenol," RSC Adv., **6**(42), pp. 35177–35190.
[70] Sheng, C., 2007, "Char Structure Characterised by Raman Spectroscopy and Its Correlations With Combustion Reactivity," Fuel, **86**(15), pp. 2316–2324.
[71] Ye, R., Xiang, C., Lin, J., Peng, Z., Huang, K., Yan, Z., Cook, N., Samuel, E., Hwang, C., Ruan, G., Ceriotti, G., Raji, A.-R., Martí, A., and Tour, J., 2013, "Coal as an Abundant Source of Graphene Quantum Dots," Nat. Commun., **4**, pp. 1–7.
[72] Chowdhury, Z. Z., Krishnan, B., Sagadevan, S., Rafique, R. F., Hamizi, N. A. B., Wahab, Y. A., Khan, A., Bin Johan, R., Al-douri, Y., Newaz Kazi, S., and Tawab Shah, S., 2018, "Effect of Temperature on the Physical, Electro-Chemical and Adsorption Properties of Carbon Micro-Spheres Using Hydrothermal Carbonization Process," Nanomaterials, **8**(8), p. 597.